
PLASMOCHEMICAL METHODS OF PRODUCTION
AND TREATMENT OF MATERIALS

Properties of a High-Power Ion Beam with Particle Energy up to 1 MeV Obtained from a Plasma Created by a High-Voltage Pulse on a Graphite Cathode

G. V. Potemkin^{a, *}, A. E. Ligachev^{b, **}, and M. V. Zhidkov^{c, ***}

^a National Research Tomsk Polytechnic University, Tomsk, 634050 Russia

^b Federal Research Center Prokhorov General Physics Institute, Russian Academy of Sciences, Moscow, 119991 Russia

^c Federal Research Center for Problems of Chemical Physics and Medicinal Chemistry, Russian Academy of Sciences, Chernogolovka, 142432 Russia

*e-mail: ep.gvp@yandex.ru

**e-mail: carbin@yandex.ru

***e-mail: zhidkov@icp.ac.ru

Received March 29, 2023; revised May 4, 2023; accepted June 26, 2023

Abstract—The features of the method for generating gas-vapor plasma and the characteristics of a high-power ion beam (HPIB) obtained in a vacuum diode with a graphite cathode using a plasma-forming high-voltage nanosecond pulse are described. The cathode material and the two-pulse mode of operation of the TEMP-4 type diode make it possible to form a multicomponent nanosecond HPIB with a maximum ion energy of up to 1 MeV, a particle flux density on the surface of $\sim 10^{13}$ ion/cm², and a power density on the sample surface of up to 10⁷ W/cm² to modify the surface properties of structural materials. Materials are published within the framework of scientific discussion. The authors invite researchers of the generation of high-power beams of non-gas ions and the processes of beam modification of solid-state materials to discuss the topics of this article.

Keywords: nanosecond high-voltage pulse, high-power ion beam, surface processing

DOI: 10.1134/S2075113324700102

INTRODUCTION

The TEMP-4 installation with a maximum energy of singly charged ions up to 1 MeV was created for modifying the surfaces of structural materials. The powerful ion beam of this installation, having a radiation pulse duration of 10–100 ns at a particle flux density of up to 10¹⁷–10¹⁸ ions/m² per pulse (10²⁴–10²⁵ ions/(m² s)) [1–4], may not only become a promising tool for materials science research but also be applied in the development of fast neutron reactors and plasma installations [5–19].

The work presents information about previously unexplained processes associated with the formation of an explosive complex plasma generated in a magnetically insulated vacuum diode [20–24] under the influence of a nanosecond high-voltage pulse (NSHVP) on a graphite cathode. The authors used experimental data on the properties of a high-power ion beam (HPIB) obtained using a Faraday cup, a Rogovskii coil, a device such as a Thomson spectrometer, and a time-of-flight device, as well as the results of their influence on the materials studied by X-ray diffraction analysis and electron microscopy.

DIODE ASSEMBLY AND MATERIALS OF CONSTRUCTION

The operation of a magnetically insulated diode operating in a two-pulse mode is based on the principle of forming a beam of ions from a plasma formed by the action of an auxiliary NSHVP on the cathode. Plasma in the discharge gap of the diode is formed as a result of explosive emission on the cathode surface [1–4, 20–24]. Graphite is currently recognized as the most effective cathode material in terms of the totality of electrophysical properties, including the maximum achievable amplitude of the beam current [1–4].

All structural graphites have porosity reaching 15–25% and anisotropy determined by a characteristic layered structure. Covalent bonds act between carbon atoms in flat hexagonal rings, while bonds between layers are formed by weak van der Waals forces. For this reason, the introduction of foreign atoms between the layers is possible, which leads to an increase in the interlayer distance. In general, structural graphite contains a large number of both macro- and microdefects, especially in the surface layer [25–28]. The volume of open pores in structural graphite is about 20%, which at normal pressure contains about 0.15 mL/g of

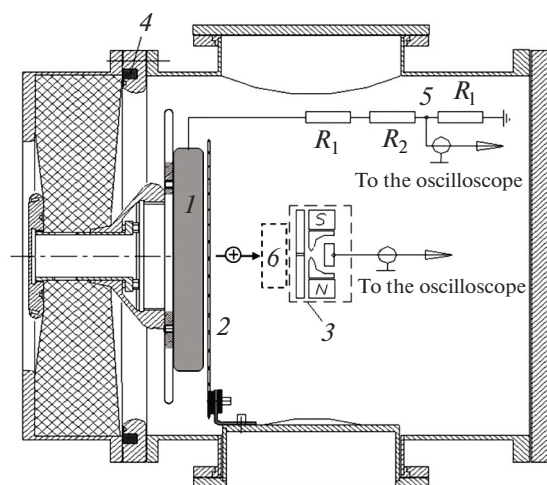


Fig. 1. Schematic of the diode assembly: (1) potential electrode of the diode (graphite), (2) grounded electrode grid, (3) collimated Faraday cup (CCF), (4) Rogowski coil, (5) voltage divider, (6) sample. The gap between the potential and grounded electrodes is 0.08 m; the distance from the grounded electrode to the CCF is 0.18 m [32].

gas. Studies of graphite degassing have shown that, at temperatures up to 1000 K, the equilibrium mixture of the gases released in a vacuum consists of H_2 and CO. At higher temperatures, the ratio of these components changes, and total vapor pressure increases from 10^{-7} Pa at 1700 K to 190 Pa at 3000 K [26, 27]. The maximum rate of gas evolution of graphite lies in the temperature range of 1100–1600 K; gas evolution is hardly observed above 2300–2500 K; however, upon contact with the atmosphere after degassing, the graphite surface is saturated again and the degree of its saturation depends on the time of contact of the graphite with the gas environment. Taking into account the fact that the gas release of structural graphite depends mainly on the presence of open porosity in the surface layer, the evaporation rate of graphite in a vacuum can be described by the equation

$$\log w = A - B/T,$$

where w is the evaporation rate ($g/(cm^2 s)$) with coefficients $A \sim 10$ and $B \sim 50000$, and T is the temperature [26, 27].

Studies of spectroscopically pure graphite vapors using a mass spectrometric method have shown that they have a complex composition, and the ratio of the components depends on temperature [26, 28]. Graphite vapors are molecular and consist mainly of C_3 . At a temperature of 2500 K, the component ratio is $C_1 : C_2 : C_3 : C_4 : C_5 = 1 : 2.8 : 4.5 : 0.35 : 0.5$. All particles included in the vapor sublimate in the form of neutral atoms or negative ions. The composition of graphite vapors sublimated under the action of laser radiation has an identical ratio of vapor components [29–31].

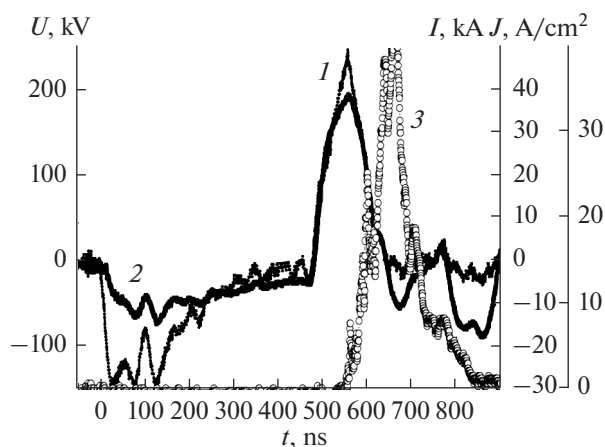


Fig. 2. Oscillograms of a self-insulating diode with flat electrodes: (1) voltage anode–cathode, U ; (2) total current of the ion beam, measured by the Rogowski coil, I ; (3) ion current density of high-power ion beam (HPIB), J [32].

Figure 1 shows a diagram of the diode assembly of the TEMP-4 installation, in which the method proposed by Yu.P. Usov's of producing plasma in the interelectrode space is implemented, when vapor–plasma formations on the surface of a potential graphite electrode are formed using an auxiliary nanosecond high-voltage pulse (NSHVP) and have a pulse duration $\tau \approx (10–100) \times 10^{-9}$ s and a voltage $U = 100–250$ kV [1–4].

Oscillograms of current and voltage of a diode operating in a double-pulse mode are presented in Fig. 2. The first pulse of negative polarity is applied to the graphite electrode 1 (Fig. 1) to form carbon plasma. The second pulse serves to accelerate positive ions of the decaying plasma. The flow of particles from the gap through a grounded electrode 2 with a transparency of 0.5 follows onto the collimated Faraday cup 3 (CFC) or onto the irradiated target. Thus, at the TEMP-4 installation, a high-power ion beam (HPIB) is obtained, which is subsequently used to study the integral effect on structural materials of high-power ion beams of solid-state materials [5–19]. Irradiation of the samples from various materials is carried out both in planar (Fig. 1) and in focusing geometry.

The samples in the vacuum chamber are changed automatically. The installation is controlled by an operator from a remote control.

EXPERIMENTAL

Depending on the purpose of using beams of charged particles, their parameters are subject to requirements for elemental composition, energy of accelerated particles, monochromaticity, and emittance, and for HPIB, the power density of the beam on the target surface [19–21, 33].

To determine the properties of HPIB of the TEMP-4 installation, the following diagnostic tools were used:

(1) Faraday cylinder (FC)—it allows one to make absolute measurements of the current of a beam of charged particles [33]; however, the possibility of using it to determine the current of HPIB is limited by the power density of the ion beam. The power density of the ion flux (Q_i) obtained at TEMP-4M according to the data from [11, 32] is

$$Q_i = \frac{\varepsilon_i n_i}{s\tau} \sim 4(10^6 - 10^8) \text{ W/cm}^2, \quad (1)$$

where ε_i is the ion energy, J; n_i is the number of ions in a pulse; s is the target area, m^2 ; and τ is duration of the radiation pulse, s. The value of Q_i for HPIB is several orders of magnitude higher than the same parameter for beams used in implantation technology (10^2 W/cm^2) and is significantly greater than the critical heat flux (q_c), which determines the destruction threshold of all metals [34].

When using a FC, it is always assumed that, under the influence of a beam of charged particles in the collector, there are no charge leaks associated with non-local phase transformations in its surface layer and changes in the electrical properties of the collector.

At the energy of charged particles $e_i = 250 \text{ keV}$, the ion flux density $N_i \sim 10^{17} - 10^{18} \text{ ion/m}^2$, and the pulse duration $\tau = 10^{-7} \text{ s}$, the specific energy e_a which an atom of a traveling iron layer of thickness $R^* = R_a + \Delta R_p$ acquires under the influence of HPIB is $e_a = \frac{\varepsilon_i N_i}{N_a} \sim$

1 eV; that is, it corresponds to the heat of evaporation for Fe [35]. Here, the number of atoms in the layer is $N_a = n_a V_1$, where n_a [atom/ m^3] and V_1 [m^3] are the atomic concentration and the volume of the traveling layer, respectively. At the specified parameters, the traveling layer of the FC absorber partially or completely evaporates, as a result of which, a vapor-plasma cloud is formed, closing the FC housing with the collector (the trailing front of the ion flow is scattered on the collector vapors) [11, 36, 37]. In addition, the HPIB obtained at the TEMP-4 installation [1–5, 22] always contains a significant proportion of undetectable neutral atoms, also making a significant contribution to thermal excitation of the collector surface. For a multicomponent beam, the shape and duration of the ion radiation pulse in this case turn out to depend on the distance between the grounded electrode of the diode and the FC (Fig. 2). The power density Q_i on the collector surface is also determined by the duration of the extended pulse t_1 , which leads to changes in the specific energy e_i [eV/atom] transferred to the traveling layer by beam particles and the amount of evaporated matter of the collector or target (1). The influence of these factors on the magnitude of the measured charge is not taken into account. The measured parameter

(the amount of collected charge) in this case turns out to depend on the HPIB power density and the length of travel of these particles R^* in the material of the FC absorber. Therefore, the collimated Faraday cylinder used in the experiments [32], for the reasons stated above, can only serve as an indicator of the magnitude of the integral current of all types of ions contained in the beam.

(2) For all problems associated with modifying the properties of a surface layer by ion beams, the issue of paramount importance is the composition of the beam and the energy spectrum of the particles incident on the surface of the sample. The source of all particles in a TEMP-4M type diode is the graphite surface facing the grounded electrode, and for ions, the volume of plasma formed inside the interelectrode space. The results of an express analysis of the elemental composition of a beam of charged particles of the TEMP-4M accelerator obtained using a device such as a Thomson spectrometer with parallel electric and magnetic fields showed the presence of carbon and hydrogen ions and impurity chemical elements from the composition of the electrode materials of the diode node in the beam [1–5].

It is known that J. Thomson developed his device for working with the plasma of a stable glow discharge of a two-component gas [38, 39]. Complex plasma [1–3, 38, 39] created by the impact of a high-voltage nanosecond pulse on the graphite surface is fundamentally different from the quiescent cold plasma of a glow discharge [34, 35], which makes the use of a Thomson-type spectrometer for mass analysis of HPIB problematic. The parameters of the constructed device (Fig. 3) given in [5] make it possible to establish its capabilities for analyzing ions by mass if the particle speed is given, defined as

$$v_i = \sqrt{\left(\frac{q_i}{m_i}\right) \sqrt{2U}}, \quad (2)$$

where q_i is the charge of the ion and m_i is mass of the ion, respectively [38, 39].

At the field induction in the spectrometer $B = 0.112 \text{ T}$, electric field strength $E = 10.7 \times 10^4 \text{ V/m}$, accelerating potential difference $U = 112 \times 10^3 \text{ V}$, and geometric parameters (Fig. 3) $l = 3 \times 10^{-2} \text{ m}$, $L = 3 \times 10^{-2} \text{ m}$, and $l(l + 2L) = 27 \times 10^{-4} \text{ m}^2$, using expressions

$$y_e = \left(\frac{q}{m}\right) E \left(\frac{l(l + 2L)}{2}\right) \left(\frac{1}{v_i^2}\right), \quad (3)$$

$$z_m = \left(\frac{q_i}{m_i}\right) l(l + 2L) B \left(\frac{1}{v_i}\right), \quad (4)$$

it is possible to obtain beam deflections along the y and z coordinates (Table 1) and plot the dependences of particle traces on the screen D (Fig. 3) in parabolic form, which merge for singly charged atomic ions of nitrogen, oxygen, and carbon, and which for triatomic single-charged C_3 and Fe^+ are barely distinguishable.

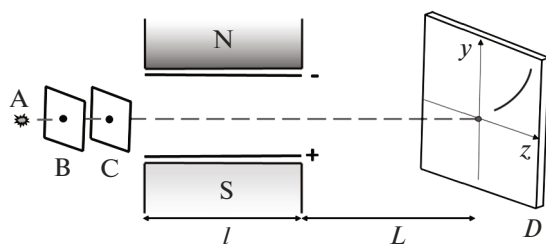


Fig. 3. Schematic of the Thomson device [5, 32]: A—ion source, B and C—diaphragms, N and S—magnet poles, ±—plates under positive or negative potential, *l*—length of capacitor plates, *L*—distance to screen *D*, *y* and *z*—coordinate axes.

Table 1 shows the speeds v_i (10^5 , m/s) and deflection of the beam particles in a plane perpendicular to the direction of motion y_e and z_m (10^{-3} , m), having passed through the parallel electric and magnetic fields of a Thomson-type device.

The presented data indicate that the used device cannot separate ions of carbon, nitrogen, and oxygen or molecular ions CH, CH₂, CO, and CO₂. All parabolas in this case merge. Focusing particles by jump angles, source sizes, and ion energy are absent in the device, and their longitudinal dispersion in energy and ratio q_i/m_i does not contribute to the separation of ions in this version of the device. The obtained mass analysis data for a graphite cathode using a Thomson device [5] indicated that the analyzed ion beam has a very wide energy spectrum of all charged particles contained in the HPIB, with a maximum energy for singly charged particles determined by the accelerating voltage. The presence of a significant fraction of protons in the beam was also established.

(3) To analyze the HPIB composition of the TEMP-4 installation, the authors of [32] also used a device with time-of-flight separation of ions in a field-free space. In this case, the time of flight t (s) of the ion distance L (m) from the plane perpendicular to the direction of motion of the ions to the collector is equal

to $t = L/v$. Taking into account Eq. (2), the expression for the time of flight takes the form

$$t = \frac{L\sqrt{m_i}}{\sqrt{2q_iU}} \tag{5}$$

For two groups of ions with different ratios q_i/m_i , the time-of-flight dispersion is equal to

$$\Delta t = \frac{L(\sqrt{m_1} - \sqrt{m_2})}{\sqrt{2q_iU}} \tag{6}$$

Expression (6) at $Dm \ll m$ takes the form

$$\Delta t = \frac{t(m_1 - m_2)}{2m} \tag{7}$$

To completely separate two ion packets with masses m_1 and m_2 so that they do not overlap, it is necessary to fulfill the Rayleigh criterion; that is, the time-of-flight dispersion of the ions must be greater than or equal to half the sum of their durations [42, 43]:

$$\Delta t > \frac{\delta t_{m_1} + \delta t_{m_2}}{2} \tag{8}$$

For the TEMP-4 vacuum diode, the authors of [32] did not determine the duration of the δt_{m_1} and δt_{m_2} packets, but their duration can be approximately judged from the oscillograms (Fig. 2). The emission of atoms and molecules from the graphite surface will occur as long as the energy of these particles is sufficient to overcome the potential barrier at the graphite–vacuum boundary. In this regard, the duration of the formation of packets of ions with mass m_i , that is, δt_{m_1} and δt_{m_2} , in a rough approximation can be set equal to the duration of the plasma-forming pulse at the base $\delta t_{m_1} = \delta t_{m_2} \sim 3 \times 10^{-7}$ s. Thus, the value $(\delta t_{m_1} + \delta t_{m_2})/2 = 3 \times 10^{-7}$ s must be less than or equal to Δt . To separate singly charged ions of atomic carbon and accompanying atomic ions of nitrogen and oxygen at a particle energy $\epsilon_i = 250 \times 10^3$ eV, the flight path length $L = \Delta t/(v_1^{-1} - v_2^{-2}) \sim 8$ m is required. For a distance $L = 0.18$ m indicated in [32], there is a merging of

Table 1. Parameters of beam particles that have passed parallel electric and magnetic fields of a Thomson-type device

$U, 10^3$ V	$q_i/m_i, 10^8$ C/kg											
	C—0.0797			N—0.0683			C ₃ —0.0398			Fe—0.017		
	v_i	y_e	z_m	v_i	y_e	z_m	v_i	y_e	z_m	v_i	y_e	z_m
5	2.8	15	4.3	2.6	14	4	2	14	3	1.3	0.1	2
15	5	4.6	2.4	4.5	4.9	2.3	3.4	5.2	1.8	2.2	0.03	1.1
25	6.3	3	1.9	5.8	2.9	1.8	4.5	2.9	1.3	2.9	0.02	0.9
50	8.9	1.5	1.4	8.2	1.5	1.3	6.3	1.3	1.0	4.1	0.01	0.6
100	12.6	1.3	1.0	11.6	0.7	0.9	8.9	0.7	0.7	5.8	0.00	0.4

Ion velocities v_i in the last line for all elements except Fe are given in 10^6 m/s.

parabolas for packets of gas ions (N^+ , CH^+ , CH^+ , O^+ , etc.) with atomic carbon C_1^+ .

(4) To describe the degree of ordering of the structure of the ion beam and the distribution of transverse velocities in the particle beam, such a characteristic as the beam emittance is used [20, 33]. No data on this characteristic of the HPIB of TEMP-4M have been published.

RESULTS AND DISCUSSION

The formation of HPIB occurs in two stages. At the first stage, after pumping out the working chamber to a pressure of $(2-5) \times 10^{-2}$ Pa, a negative nanosecond high-voltage pulse is applied to a potential graphite electrode. As a result of the interaction of NSHVP with the surface layer of graphite, a plasma-like environment is formed, consisting of neutral and partially ionized atoms and molecules of carbon and gases, contained in the surface layer of graphite. At the second stage, after a period of time, approximately equal to the pulse duration of the first negative NSHVP, a positive nanosecond high-voltage pulse is applied to the same graphite electrode. Positive ions of the decaying plasma are pushed toward the grounded grating electrode and fall onto a target or a measuring device (Fig. 1), and particles with a negative charge drift back to the graphite electrode. The energy acquired by positively charged particles in the discharge gap during the action of NSHVP, in this case, will depend on the time and place of ionization of atoms and molecules of carbon and gases; therefore, the HPIB will have a wide energy spectrum of accelerated ions.

The decisive role in the formation of a plasma-like environment in the discharge gap of the TEMP-4 diode and the subsequent formation of HPIB is played by the process of interaction of the first plasma-forming nanosecond high-voltage pulse with the surface of the graphite electrode. The formation of a vapor-gas atmosphere above its surface occurs as a result of thermal desorption of gases and sublimation of carbon particles. The expected composition of the plasma, from which the HPIB is formed in the TEMP-4 accelerator, can be judged by the types of particles leaving the surface of the graphite electrode under the influence of the plasma-forming NSHVP. Regarding graphite, it is necessary to note that the sources of atoms, molecules, and clusters of carbon and absorbed atoms and molecules of gases and water vapor are the interlayer spaces and pores of the surface layer of graphite, as well as nanoobjects of various shape on the working surface of the electrode. Desorption of gases from the surface of electrodes under the influence of high-voltage pulses was studied previously from the point of view of its effect on breakdown and insulation. The dependence of the amount of desorbed gas on the steepness of the leading edge of a

high-voltage pulse has been established in [44], but the influence of high-voltage pulses in the nanosecond range on the rate of release and the magnitude of flows of desorbed gases was not determined. The process of desorption of gases and sublimation of carbon particles under the influence of NSHVP depends mainly on the state of the surface layer of the electrode. The real surface of the electrodes is characterized by microgeometry, which describes protrusions and depressions contained on the surface. The properties of the rough layer are assessed using the parameter R_z , which is the sum of the height of the largest protrusion of the profile (R_p) and the depth of the largest depression of the profile (R_v) within the base length [45]. In the same layer, as a rule, the maximum of macro- and microdefects, both physical and chemical, is concentrated [26, 46, 47]. As for materials used in electronics, information about the microrelief of the electrode surface will not be complete in the absence of the data on sub-roughness (Fig. 4). In this case, sub-roughness, indicating the presence of nanoobjects on the surface, according to [45], depends mainly on the grain size of the material. The presence of irregularities on the graphite surface, with characteristic sizes of tens and hundreds of nanometers, is a necessary condition for the emission of electrons in both pointed and nonedged forms of nanocarbon [48–51].

In terms of its electrical properties, graphite is classified as a semimetal with a frequency-dependent dielectric constant ϵ . For graphite in the frequency range of 10^4-10^8 Hz, dielectric constant $\epsilon = 16.5$, magnetic permeability $\mu = \mu_0 = 4\pi \times 10^{-7}$ H/m, and specific conductivity $\sigma = 0.13 \times 10^6$ S/m (without taking into account anisotropy). In this case, part of the energy of the package of electromagnetic waves in the form of NSHVP (Fig. 2) is converted into Joule heat. The characteristic roughness dimensions R_p and R_z of the electrodes made from graphite by mechanical processing coincide in order of magnitude with the depth of the skin layer for the frequency band corresponding to the leading edge of nanosecond pulses. A rough estimate of the skin layer for a massive body can be obtained using the relation [52]

$$\delta = \sqrt{\frac{2}{\omega\mu\sigma}} = \frac{1}{\sqrt{\pi\mu_0\mu\sigma f}} \approx 0.3 \times 10^{-4} \text{ m} \sim R_z, \quad (9)$$

where $\omega = 2\pi f \sim 10^8$ Hz is the frequency of electronic waves of the leading edge of a nanosecond high-voltage pulse with a plasma-forming pulse duration of $\tau = 10^{-7}$ s [34, 52], and f is the cyclic frequency. The imperfection of the surface prevents purely tangential flow of current and effectively reduces conductivity of the surface; that is, the actual thickness of the skin layer will be less than that indicated in expression (9).

Under the influence of a negative nanosecond high-voltage pulse in the surface layer of graphite, part of the energy of the wave packet is transferred to conduction electrons and phonons, which in turn interact

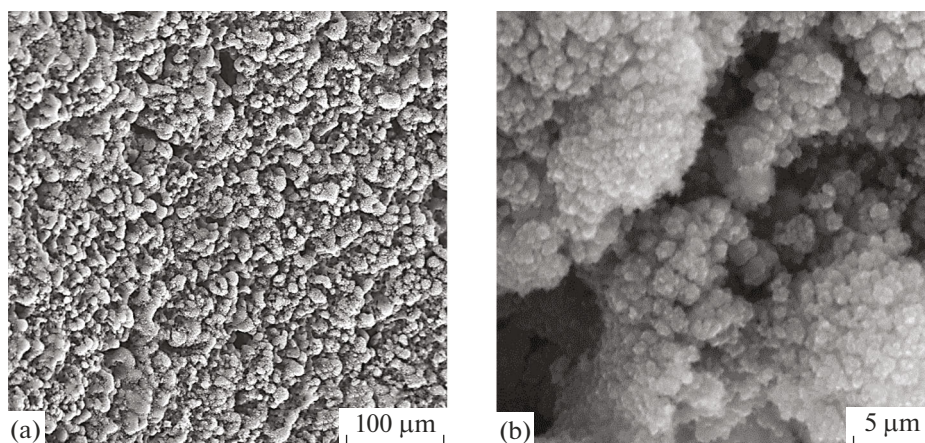


Fig. 4. Microgeometry of a rough graphite surface after machining.

with each other [44, 51, 53]. The result of their interaction is a change in the initial energy spectrum of conduction electrons and an increase in the concentration of the particles with energies above the Fermi energy near the graphite–vacuum interface. Interaction of “hot” electrons and phonons formed under the influence of NSHVP with static defects, the content of which is maximal in a layer with thickness $\sim R_z$, leads to heating of the graphite lattice [26, 53]. Volumetric thermal conductivity of graphite at low temperatures (up to ~ 400 K) is ensured by energy transfer by phonons (the Wiedemann–Franz ratio for graphite is 100 times higher than the classical value), and at higher temperatures ($T > 10^3$ K), the transfer occurs jointly with conduction electrons, and the thermal conductivity drops sharply after $\sim 5 \times 10^3$ K. The impact of a nanosecond high-voltage pulse in the skin layer is similar to a thermal shock owing to the high rate of the temperature rise, since $\sim 70\%$ of the electromagnetic energy is absorbed in the δ -layer with a frequency ω during the relaxation time of the electric field $\tau \sim \epsilon/\sigma$ [34, 52]. Thermal shock eliminates interstitial gas compounds from the interlayer space of graphite and forms areas of nanoporous carbon, which exhibits the ability for low-voltage electron emission [48–51]. The interaction of the plasma formed under the influence of NSHVP with the graphite surface also contributes to the formation of such regions [48–51].

The main role in the occurrence of electron emission under the influence of NSHVP from the surface of a graphite cathode is played by emission centers present on the working surface of the electrode in the form of nanoobjects, nanopores of the surface layer [46–51], and whiskers [22, 24, 51]. Intense properties of a substance with the surface nanoobjects with dimensions less than 100 nm (density, electrical and thermal conductivity, diffusion coefficient, etc.) already depend on their size or volume; that is, they become extensive and do not coincide with macroscopic ones [42, 47]. The presence of irregularities on

the graphite surface, with characteristic dimensions of tens and hundreds of nanometers, is a sufficient condition for emission of electrons in both pointed and non-edged forms of nanocarbon. The reason for electron emission can simultaneously be the strengthening of the applied field at the tips of morphological surface elements with a high geometric aspect ratio and low-voltage emission from non-edged structures with a relatively smooth surface [48–51]. If the internal electrons are not in thermodynamic equilibrium (which is typical of the skin layer of a graphite electrode during the action of a nanosecond high-voltage pulse), then the emission current is partially or completely determined by the supply of electrons to the radiation region. At the same time, the greater part of electrons leaves the surface by tunneling, but is not accurately described by a Fowler–Nordheim type equation [48–51].

The picture of the process of formation of gas-carbon plasma is determined by the rates of particle release dN/dt during thermal desorption of gases and sublimation of carbon particles moving from the surface of the graphite electrode at velocities about $v = \frac{\sqrt{k_B T}}{m}$ (T is absolute temperature, K; m is the particle mass; k_B is the Boltzmann constant) and changes in the spectral density of conduction electrons in the skin layer under the action of a nanosecond high-voltage pulse. Some idea of the first process is given by the shape of the current pulse for negative NSHVP. In accordance with the depths of potential wells for physical adsorption, thermal energy ($\sim 25 \times 10^{-3}$ eV), and chemical absorption (~ 1 eV), first, atoms and molecules of polymolecular adhesion layers associated with the graphite surface weakly by van der Waals forces will leave the electrode surface [54, 55]. As the voltage amplitude of the NSHVP increases, the lattice temperature increases, and gas interstitial compounds evaporate from the interlayer spaces of graphite. The centers of sublimation of carbon particles and the

release of gases are randomly distributed on the surface of the graphite electrode, as well as the centers of electron emission. Their location changes with increasing voltage at the leading edge of the pulse (Fig. 2), and the number of these centers increases with increasing voltage up to U_{\max} . The pressure in the TEMP-4 working chamber during the interaction of a nanosecond high-voltage pulse with graphite jumps by several orders of magnitude and quickly drops to a working value of $\sim 10^{-2}$ Pa after the end of the pulse.

The recorded pressure of carbon vapor of $\sim 10^{-8}$ Pa for equilibrium conditions is achieved already at a temperature of $T \sim 1600$ K. The presence of nanoobjects on the graphite surface, as well as the action of the skin effect, makes it possible to achieve similar vapor elasticity owing to size effects at noticeably lower temperatures. In this case, the predominant part of the vapor will continue to be C_3 molecules [26, 30, 31]. The contribution of ponderomotive forces to the composition of carbon vapors lies in the appearance of carbon clusters and macroparticles in them, which is confirmed by the X-ray diffraction analysis data of irradiated samples [11]. The specific effects of the TEMP-4 installation are (a) periodic saturation of the graphite electrode of the diode with water vapor and atmospheric gases (each time the working chamber is opened) and (b) mass transfer between a grounded stainless steel electrode and a potential graphite electrode (during irradiation of the samples) [56]. The influence of chemical components of the stainless steel deposited on the graphite electrode owing to mass transfer during operation of the diode affects desorption of gases and emission of electrons from the surface [54, 55, 57], but the extent of this influence is unknown.

As already noted, under the influence of NSHVP, gases are desorbed from the surface layer of the graphite electrode both in the form of atoms and molecules and in the form of ions. The effect of a negative NSHVP on a graphite electrode also leads to the appearance of a noticeable fraction of negative carbon ions in the flow of sublimated carbon particles [29–31]. The product of interaction of the flows of sublimated carbon particles and desorbed atoms and molecules of gases with the flows of ionizing electrons will be gaseous carbon plasma. Such plasma is complex, since it contains a significant amount of particles with different values of q_i/m_i . [40, 41]. Elemental analysis data of the irradiated samples within the projective path systematically showed the presence of comparable amounts of nitrogen and oxygen atoms in the layer under study, in addition to carbon [11, 19] (Figs. 5, 6).

The formation of a plasma-like medium by the action of a negative NSHVP on the graphite surface in [1–3] is not an equilibrium process and does not follow the laws of classical nonequilibrium thermodynamics [58]. The approaches and expressions used to describe this medium in [32] do not reflect its real

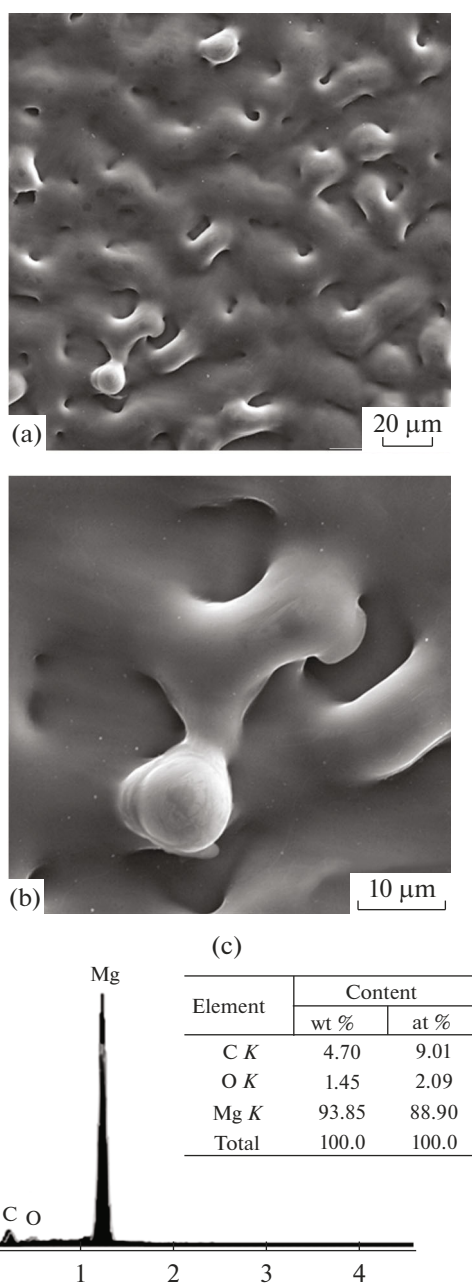


Fig. 5. Topography (a, b) and elemental composition (c) of the magnesium surface after HPIB processing (3 J/cm^2 , 10 pulses). (a, b) Scanning electron microscopy [19].

properties. Analysis of the processes of formation of gas-carbon plasma requires the use of modern ideas and concepts about the evolution of atomic-molecular structures of the nanosystems existing on the surface of the electrode under the influence of nanosecond high-voltage pulses, as well as behavior of countable ensembles of particles such as nanoobjects from the standpoint of extended irreversible thermodynamics [46, 47, 58]. The issue of the formation of a plasma-like medium in the discharge gap during the interac-

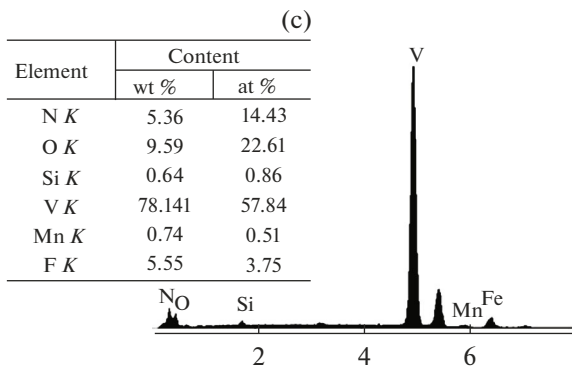
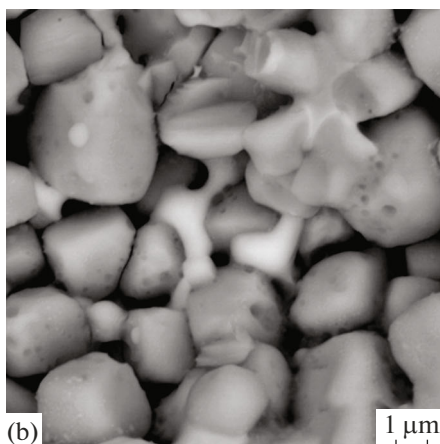
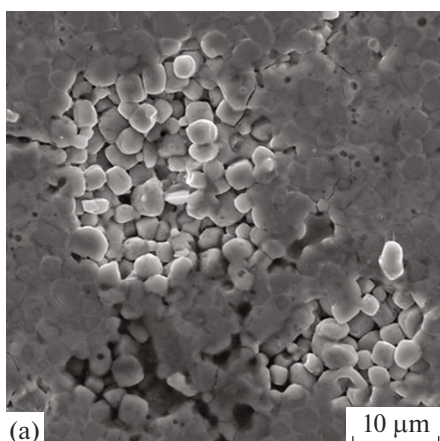


Fig. 6. Topography (a, b) and elemental composition (c) of the ferrovanadium surface after HPIB treatment. (a, b) Scanning electron microscopy [11].

tion of the NSHVP with a graphite electrode is key to obtaining a technological ion beam intended for modifying the physical and mechanical properties of the parts made of structural materials (especially this concerns processing of metals and alloys) [11]. The presence of gas ions, and especially oxygen, in the HPIB, as a rule, in most cases has a negative effect on the properties of the surface and subsurface layer of metallic materials [59].

CONCLUSIONS

A powerful beam of carbon ions with particle energy up to 1 MeV, simultaneously combining the ability of energy impact owing to introduction of a specific energy of about 1 eV/atom into the running layer and a chemical effect owing to introduction of carbon impurities up to 0.1 at %, is a unique tool both for materials science research and technological application.

The technological process of modifying physical, chemical, and operational properties of the surface layer of materials with a thickness of approximately $2R_z$ using TEMP-4 type installations is quite simple and does not require significant costs. The diode system of the installation allows operation in planar and focusing geometries, thereby providing the ability to regulate the beam size and current density on the target.

Since the main consumables are graphite, vacuum oil, and electricity, as well as replaceable elements of vacuum and electrical equipment, the costs of introducing the technology are determined mainly by the cost of the installation. Depending on the sample material, from several to tens of radiation pulses of a given energy and ion current density are required to change the surface properties.

The scope of application of high-power ion beams can be significantly expanded, and the efficiency of the surface treatment of materials can be increased by improving the quality of the TEMP-4 HPIB.

ACKNOWLEDGMENTS

The authors thank Prof. G. E. Remnev, Doctor of Engineering Sciences, for many years of support of experiments on the effects of high-power ion beams on structural materials and useful discussions of previously published results.

FUNDING

This work was supported by ongoing institutional funding. No additional grants to carry out or direct this particular research were obtained.

CONFLICT OF INTEREST

The authors of this work declare that they have no conflicts of interest.

REFERENCES

1. Logachev, E.I., Remnev, G.E., and Usov, Yu.P., Heavy ion accelerator, *Prib. Tekh. Eksp.*, 1983, no. 1, pp. 21–23.
2. Logachev, E.I., Remnev, G.E., and Usov, Yu.P., Acceleration of ions from explosive emission plasma, *Pis'ma Zh. Tekh. Fiz.*, 1980, vol. 6, no. 22, pp. 1404–1406.
3. Logachev, E.I., Remnev, G.E., and Pechenkin, S.A., Investigation of beam divergence and homogeneity of

- heavy ion emission under direct acceleration, *Zh. Tekh. Fiz.*, 1984, vol. 10, pp. 2027–2029.
4. Isakov, I.F., Kolodii, V.N., Opekunov, M.S., Matvienko, V.M., Pechenkin, S.A., Remnev, G.E., and Usov, Yu.P., Sources of high power ion beams for technological applications, *Vacuum*, 1991, vol. 42, no. 1/2, pp. 159–162.
[https://doi.org/10.1016/0042-207X\(91\)90101-N](https://doi.org/10.1016/0042-207X(91)90101-N)
 5. Pogrebnyak, A.D., Remnev, G.E., Chistyakov, S.A., and Ligachev, A.E., Modification of the properties of metals by high-power ion beams, *Sov. Phys. J.*, 1987, vol. 30, pp. 39–48.
<https://doi.org/10.1007/BF00896012>
 6. Didenko, A.N., Ligachev, A.E., and Kurakin, I.V., *Vozdeistvie puchkov zaryazhennykh chastits na poverkhnosti metallov i splavov* (Effect of Charged Particle Beams on the Surface of Metals and Alloys), Moscow: Energoatomizdat, 1987.
 7. Uglov, V.V., Remnev, G.E., Kuleshov, A.K., Astashinski, V.M., and Saltymakov, M.S., Formation of hardened layer in WCTiC–Co alloy by treatment of high intensity pulse ion beam and compression plasma flows, *Surf. Coat. Technol.*, 2010, vol. 204, nos. 12–13, pp. 1952–1956.
<https://doi.org/10.1016/j.surfcoat.2009.09.039>
 8. Korotaev, A.D., Tyumentsev, A.N., Pochivalov, Yu.I., Ovchinnikov, S.V., Remnev, G.E., and Isakov, I.F., Phase composition and defect structure in the surface layer of metal targets irradiated by high power ion beams, *Phys. Met. Metallogr.*, 1996, vol. 81, no. 5, pp. 542–548.
<https://www.elibrary.ru/item.asp?id=14937041>
 9. Kovivchak, V.S., Krivozubov, O.V., Leont'eva, N.N., and Knyazev, E.V., Structural phase transformations in tin dioxide under the action of a nanosecond high-power ion beam, *Tech. Phys. Lett.*, 2013, vol. 39, pp. 982–985.
<https://doi.org/10.1134/S1063785013110229>
 10. Galkin, N.G., Vavanova, S.V., Galkin, K.N., Batalov, R.I., Bayazitov, R.M., and Nuzhdin, V.I., Pulsed nanosecond annealing of magnesium-implanted silicon, *Tech. Phys.*, 2013, vol. 58, no. 1, pp. 94–99.
<https://doi.org/10.1134/S1063784213010064>
 11. Potemkin, G.V., Syrtanov, M.S., Lepakova, O.K., Kitler, V.D., Ligachev, A.E., and Zhidkov, M.V., Phase transformations in nitrided ferrovanadium under the action of a high power carbon ion beam, *Inorg. Mater.: Appl. Res.*, 2021, vol. 12, no. 3, pp. 615–624.
<https://doi.org/10.1134/S207511332103031X>
 12. Davis, H.A., Remnev, G.E., Stinnett, R.W., and Yatsui, K., Intense ion-beam treatment of materials, *MRS Bull.*, 1996, vol. 21, no. 8, pp. 58–62.
 13. Yatsui, K., Kang, X.D., Sonogawa, T., Matsuoka, T., Masugata, K., Shimotori, Y., Satoh, T., Furuuchi, S., Ohuchi, Y., Takeshita, T., and Yamamoto, H., Applications of intense pulsed ion beam to materials science, *Phys. Plasmas*, 1994, vol. 1, no. 5, pp. 1730–1737.
 14. Remnev, G.E. and Shulov, V.A., Application of high-power ion beams for technology, *Laser Part. Beams*, 1993, vol. 11, no. 4, pp. 707–731.
 15. Mei, X.X., Sun, W.F., Hao, S.Z., Ma, T.C., and Dong, C., Surface modification of high-speed steel by intense pulsed ion beam irradiation, *Surf. Coat. Technol.*, 2007, vol. 201, nos. 9–11, pp. 5072–5076.
 16. Shulov, V.A., Remnev, G.E., and Nochovnaya, N.A., Phenomenon crater formation in the interaction of powerful ion beams with the surface of metals and alloys: General characteristics, *Poverkhn.: Fiz., Khim., Mekh.*, 1993, no. 12, pp. 110–121.
 17. Remnev, G.E., Tarbokov, V.A., and Pavlov, S.K., Material modification by powerful pulsed ion beams, *Inorg. Mater.: Appl. Res.*, 2022, vol. 13, no. 3, pp. 626–640.
<https://doi.org/10.1134/S2075113322030327>
 18. Zhidkov, M.V., Ligachev, A.E., Golosov, E.V., Gazizova, M.Y., Pavlov, S.K., and Remnev, G.E., Study of craters formed on surface of AISI 321 stainless steel after high power ion-beam exposure, *Vacuum*, 2022, vol. 198, p. 110852.
<https://doi.org/10.1016/j.vacuum.2021.110852>
 19. Potemkin, G.V., Ligachev, A.E., Zhidkov, M.V., Kolobov, Yu.R., Remnev, G.E., Gazizova, M.Yu., Bozhko, S.A., and Bureev, O.A., Change of magnesium surface topography under the action of a powerful pulsed ion beam, *Fiz. Khim. Obrab. Mater.*, 2015, no. 4, pp. 5–9.
 20. Bystritskii, V.M. and Didenko, A.N., *High Power Ion Beams*, New York: Am. Inst. Phys., 1990.
 21. Lawson, J.D., *The Physics of Charged-Particle Beams*, Oxford: Clarendon, 1977.
 22. Miller, R.B., *An Introduction to the Physics of Intense Charged Particle Beams*, New York: Springer, 1982.
 23. Mesyats, G.A., *Generirovanie moshchnykh nanosekundnykh impul'sov* (Generation of Powerful Nanosecond Pulses), Moscow: Sov. Radio, 1974.
 24. Mesyats, G.A., *Vzryvnaya elektronnaya emissiya* (Explosive Electron Emission), Moscow: Fizmatlit, 2011.
 25. Ubbelohde, A. and Lewis, F.A., *Graphite and Its Crystal Compounds*, Oxford: Clarendon, 1960.
 26. Ostrovskii, V.S., Virgil'ev, Yu.S., Kostikov, V.I., and Shipkov, N.N., *Iskusstvennyi grafit* (Artificial Graphite), Moscow: Metallurgiya, 1986.
 27. Zhmurikov, E.I., Bubnenkov, I.A., Dremov, V.V., Samarin, S.I., Pokrovskii, A.S., and Khar'kov, D.V., *Grafit v nauke i yadernoi tekhnike* (Graphite in Science and Nuclear Engineering), Novosibirsk: Sib. Branch Russ. Acad. Sci., 2013.
 28. Gubin, S.P. and Tkachev, S.V., *Grafen i rodstvennyye nanoformy ugleroda* (Graphene and Related Carbon Nanoforms), Moscow: Librocom, 2012.
 29. Honig, R., Mass spectrometric study of the molecular sublimation of graphite, *J. Chem. Phys.*, 1954, vol. 22, no. 1, pp. 126–131. <https://doi.org/10.1063/1.1739819>
 30. von Helden, G., Hsu, M.T., Gotts, N., and Bowers, M.T., Carbon cluster cations with up to 84 atoms: Structures, formation mechanism, and reactivity, *J. Phys. Chem.*, 1993, vol. 97, pp. 8182–8192.
<https://doi.org/10.1002/chin.199345033>
 31. Joseph, M., Sivakumar, N., and Manoravi, P., High temperature vapor pressure studies on graphite using laser pulse heating, *Carbon*, 2002, vol. 40, no. 11, pp. 2021–2040.
[https://doi.org/10.1016/S0008-6223\(02\)00158-6](https://doi.org/10.1016/S0008-6223(02)00158-6)

32. Pushkarev, A.I. and Isakova, Yu.I., *Diagnostika moshchnykh ionnykh puchkov: Monografiya* (Diagnostics of High-Power Ion Beams: Monograph), Novosibirsk: ANS SibAK, 2016.
33. Moskalev, V.A. and Sergeev, G.I., *Izmerenie parametrov puchkov zaryazhennykh chastits* (Measurement of Parameters Charged Particle Beams), Moscow: Energoatomizdat, 1991.
34. Veiko, V.P., Libenson, M.N., Chervyakov, G.G., and Yakovlev, E.B., *Vzaimodeistvie lazernogo izlucheniya s veshchestvom* (Interaction of Laser Radiation with Matter), Moscow: Fizmatlit, 2008.
35. Kittel, C., *Introduction to Solid State Physics*, New York: Wiley, 1976.
36. Humphries, S.J., Maenchen, S., and Sudan, R.N., Measurements of 400 MW/cm² proton fluxes, *J. Appl. Phys.*, 1977, vol. 48, no. 4, pp. 1449–1455.
37. Young, F.C., Golden, J., and Kapetanakis, C.A., Diagnostics for intense pulsed ion beams, *Rev. Sci. Instrum.*, 1977, vol. 37, no. 1, pp. 21–25.
38. Shpol'skii, E.V., *Atomnaya fizika* (Atomic Physics), Moscow: Nauka, 1974, vol. 1.
39. Dobretsov, L.N., *Atomnaya fizika* (Atomic Physics), Moscow: Gosizdat, 1960.
40. Fortov, V.E., Khrapak, A.G., and Yakubov, I.T., *Fizika neideal'noi plazmy* (Physics of Non-Ideal Plasma), Moscow: Fizmatlit, 2004.
41. Bouchoule, A., *Dusty Plasmas: Physics, Chemistry and Technological Impacts in Plasma Processing*, Chichester: Wiley, 1999.
42. Rick, T.R., *Mass-spektroskopiya* (Mass Spectroscopy), Moscow: Gostekhzdat, 1953.
43. Sysoev, A.A. and Chupakhin, M.S., *Vvedenie v mass-spektrometriyu* (Introduction to Mass Spectrometry), Moscow: Atomizdat, 1977.
44. Slivkov, I.N., *Elektroizolyatsiya i razryad v vakuume* (Electrical Insulation and Vacuum Discharge), Moscow: Atomizdat, 1972.
45. Suslov, A.G., Poroshin, V.V., Shalygin, M.G., and Kuznetsov, S.V., Relationship of nanoroughness (sub roughness of workpiece surface and material grain size), *Naukoemkie Tekhnol. Mashinostr.*, 2015, no. 11, pp. 3–7.
46. Golovin, Yu.I., *Osnovy nanotekhnologii* (Fundamentals of Nanotechnology), Moscow: Mashinostroenie, 2012.
47. Roduner, E., *Nanoscope Materials: Size-Dependent Phenomena*, Cambridge: R. Soc. Chem., 2006.
48. Sheshin, E.P., *Struktura poverkhnosti i avtoemissionnye svoistva uglerodnykh materialov* (Surface Structure and Autoemission Properties of Carbon Materials), Moscow: Moscow Inst. Phys. Technol., 2001.
49. Obraztsov, A.N., Volkov, A.P., Boronin, A.I., and Koshcheev, S.V., Rehybridization of the atomic orbitals and the field electron emission from nanostructured carbon, *J. Exp. Theor. Phys.*, 2001, vol. 93, pp. 846–852.
<https://doi.org/10.1134/1.1420454>
50. Elets'kii, A.V., Carbon nanotube-based electron field emitters, *Phys.-Usp.*, 2010, vol. 53, no. 9, pp. 863–892.
<https://doi.org/10.3367/UFNe.0180.201009a.0897>
51. Shishkin, G.G. and Ageev, I.M., *Nanoelektronika: Elementy, pribory, ustroystva* (Nanoelectronics: Elements, Instruments, Devices), Moscow: Binom, 2011.
52. Pain, H.J., *The Physics of Vibrations and Waves*, Chichester: Wiley, 1976.
53. Brandt, N.B. and Kul'bachinskii, V.A., *Kvazichastitsy v fizike kondensirovannogo sostoyaniya* (Quasiparticles in Condensed Matter Physics), Moscow: Fizmatlit, 2005.
54. Pratton, M., *Introduction to Surface Physics*, Oxford: Clarendon, 1994.
55. Zangwill, A., *Physics at Surfaces*, Cambridge: Cambridge Univ. Press, 1988.
56. Pavlov, S.K., Ligachev, A.E., Potemkin, G.V., and Remnev, G.E., Mass transfer between electrodes of a magnetically insulated diode operating in a two-pulse mode, *Materialy XI mezhdunarodnoi konferentsii "Vzaimodeistvie izlucheniya s tverdyim telom"* (Minsk, Belarus', 23–25 sentyabrya 2015) (Proc. XI Int. Conf. "Interaction of Radiation with Solid State" (Minsk, Belarus, September 23–25, 2015)), Minsk: Belarus State Univ., 2015, pp. 419–421.
57. Berry, R.S. and Smirnov, B.M., Phase transitions in various kinds of clusters, *Phys.-Usp.*, 2009, vol. 52, no. 2, pp. 137–164.
<https://doi.org/10.3367/UFNe.0179.200902b.0147>
58. Jou, D., Casas-Vazquez, J., and Lebon, G., *Extended Irreversible Thermodynamics*, Berlin–Heidelberg: Springer-Verlag, 2001.
<https://doi.org/10.1007/978-3-642-56565-6>
59. Hocking, M.G., Vasantasree, V., and Sidky, P.S., *Metallic and Ceramic Coatings: Production, High Temperature Properties and Applications*, London: Longman, 1989.

Translated by Sh. Galyaltdinov

Publisher's Note. Pleiades Publishing remains neutral with regard to jurisdictional claims in published maps and institutional affiliations.